J Fluoresc (2014) 24:455–463
DOI 10.1007/s10895-013-1311-x

ORIGINAL PAPER

# Probing solute-solvent interaction in 1-ethyl-3-methylimidazolium-based room temperature ionic liquids: A time-resolved fluorescence anisotropy study

**Sudhir Kumar Das · Moloy Sarkar**

Received: 17 July 2013 / Accepted: 9 October 2013 / Published online: 26 October 2013


**Abstract** Rotational diffusion of two organic solutes, coumarin153 (C153) and 4-aminophthalimide (AP) has been investigated in four ionic liquids (ILs), viz. 1-ethyl-3-methylimidazolium trifluoroacetate (EMIMTFA), 1-ethyl-3-methylimidazolium ethylsulfate (EMIMESU), 1-ethyl-3-methylimidazolium tetrafluoroborate (EMIMTFB) and 1-ethyl-3-methylimidazolium tetracyanoborate (EMIMTCB), as a function of temperature. Between the two probes, AP can act as hydrogen-bond-donor to the solvents having hydrogen bond acceptor ability. The results indicate that the rotational dynamics of C153 is mainly governed by the viscosity of the medium. On the other hand, the rotational motion of AP is found to be significantly hindered in the ILs depending on the nature of anions of the ILs. Rotational coupling constant values for AP in the ILs follow the order TFA>ESU>TCB> TFB. The slower rotational motion of AP in these ILs has been attributed to the specific hydrogen bonding interaction between AP and anions of ILs.

**Keywords** Ionic liquids · Fluorescence · Anisotropy · Anion dependence · Specific interaction

## Introduction

Ionic liquids have received considerable attention in recent times due to their applications in diverse areas of chemistry and biology [1–7]. This is mainly because of their unique physicochemical properties [6, 7]. Intermolecular interactions play an important role in determining the physicochemical properties of liquids and solutions. It is, therefore, worthwhile to probe the various natures of interactions that exist between the constituents of the ILs and also their interaction with added solutes so that we can comprehend, and even predict their physicochemical properties [8–37].

Many experimental and theoretical investigations have been carried out in ILs in recent times basically to understand the molecular origin of solvent-solvent, solute-solvent interactions [8–38] and charge/electron transfer processes [38, 39]. Studies on the rotational relaxation behavior of organic solutes were found to be useful to understand specific solute-solvent interactions [40]. Maroncelli and co-workers [15, 16] have demonstrated that the rotational dynamics of organic solutes are mainly controlled by viscosity of the medium and are independent of the electrostatic and/or specific hydrogen bonding interactions. Subsequently, other researchers including ourselves have found that rotational motion of organic solutes in ionic liquids is significantly hindered due to specific solute-solvent interaction [27–36].

It is evident from the earlier reports that although the experimentally measured reorientation times generally lie between the broad limits of slip and stick hydrodynamic boundary conditions [41], a perfect match has not often been achieved and significant deviations from normal hydrodynamic conditions have also been observed. In this context, it may be mentioned that according to the stick boundary condition, the tangential velocity of the fluid relative to the body vanishes on the surface of the body and there exists a perfect coherence between the motion of the body and the surrounding fluid [41]. On the other hand, in slip boundary condition the fluid exert no tangential stress on the rotating objects [41]. It has also been found that the systematic variation of the constituents can tune the physical properties of ILs, and this attribute is also expected to influence the solute-solvent interaction in a systematic manner. Hence, the study of the rotational behavior of organic solutes in the ILs by maintaining a systematic variation in the constituent of the IL is expected to

S. K. Das · M. Sarkar (✉)
School of Chemical Sciences, National Institute of Science Education and Research, Bhubaneswar 751005, India
e-mail: moloysarkar@gmail.com

throw more light on the role of solute-solvent interaction towards the departure of rotational behavior of these solutes from that of the normal hydrodynamic predictions. It is pertinent to mention in this context that Xu and co-workers [8] have recently shown that H-bonding interaction is the most dominant interaction of ILs governing the solubility of flavonoids, and the anionic part has greater effect on the overall H-bonding ability of the ionic liquids. The authors have determined the hydrogen bond basicity of 32 anion components of ionic liquids and classified them into three groups (higher, medium and lower) depending upon the hydrogen bond basicity of the anions. Keeping this in mind, we have studied rotational diffusion of two neutral organic solutes, 4-aminophthalimide (AP) and coumarin 153 (C153) in four different ionic liquids, viz. 1-ethyl-3-methylimidazolium trifluoroacetate (EMIMTFA), 1-ethyl-3-methylimidazolium ethylsulfate (EMIMESU), 1-ethyl-3-methylimidazolium tetrafluoroborate (EMIMTFB) and 1-ethyl-3-methylimidazolium tetracyanoborate (EMIMTCB). These ILs are purposefully chosen so that an appreciable variation of the hydrogen bond basicity in the ILs is achieved. In all ILs under study, a fixed cationic moiety is used so that the effect of anions on the rotational dynamics is exclusively monitored. Both these probes are suitable for rotational dynamics study in organic medium [17, 27]. Among these probes, only AP has the hydrogen-bond-donating ability by virtue of its polarized N-H fragment [27]. Structural information on the solutes and the ionic liquids are provided in Chart 1.

## Materials and experimental technique

4-Aminophthalimide (AP) was obtained from TCI and recrystalized from ethanol. The purity of the compound was confirmed by performing thin layer chromatography and NMR spectral measurements. Coumarin 153 (C153) (laser grade, Exciton) was used as received. The ionic liquids were obtained from the Merck Germany (>99 % purity). The water and halide contents of the ILs were <100 ppm. The ILs were kept overnight in high vacuum to remove any moisture present in these media. Proper precaution is taken to avoid moisture absorption by the media during transferring the solute into a cuvette.

The viscosities (η) of the ILs were measured by using an LVDV-III Ultra Brookfield Cone and Plate viscometer (1 % accuracy and 0.2 % repeatability). Time-resolved anisotropy decay measurements were carried out using a time-correlated single photon counting (TCSPC) spectrometer (Edinburgh, OB920). A diode laser (405 nm) was used as the excitation source, and signals were collected at magic angle (54.7°) by using an MCP photomultiplier (Hamamatsu R3809U-50) as the detector (response time 40 ps). The instrument response function of the experimental set up was limited by the full width half maxima (FWHM) of the excitation laser pulse, and was 95 ps for 405 nm laser diode. The instrument response function (IRF) was recorded by scatterer (dilute ludox solution in water) in place of the sample. For excitation and emission, M100-X monochromators (Seya-Namioka; 2 nm band pass) were used. Time resolved fluorescence anisotropy decay

**Chart 1** Molecular diagrams of solutes and solvents used in the study

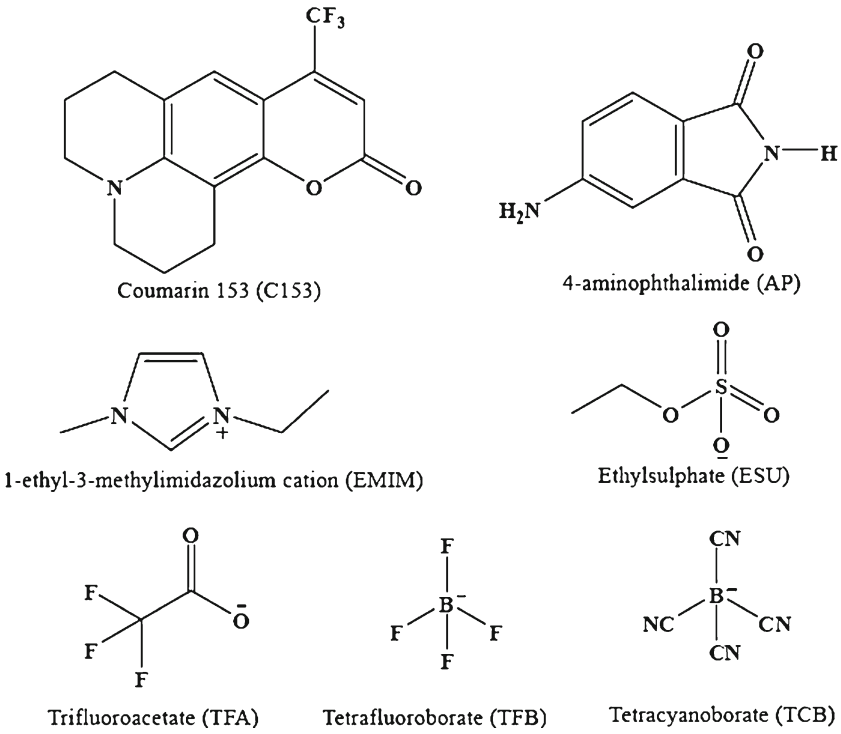

profiles were analyzed by a non-liner least-square iteration procedures using F900 decay analysis software. The criteria for a good fit were judged by statistical parameters such as the reduced $\chi^2$ being close to unity and the random distribution of the weighted residuals. The temperature was controlled by circulating water through the cell holder using a Quantum, North West (TC 125) temperature controller with the accuracy ±0.2 °C. Waiting time was half an hour for each measurement. The time-resolved fluorescence anisotropy measurement was done by using two polarizer by placing one of them in the excitation beam path and the other one in front of the detector. An alternate collection of the fluorescence intensity in parallel and perpendicular polarization (with respect to the vertically polarized excitation laser beam) for equal interval of time was carried out. For G-factor calculation, the same procedure was followed but with horizontal polarization of the exciting laser beam.

## Results and discussion

The time resolved fluorescence anisotropy, $r$, is estimated by employing the following equation

$$r = \frac{I_{VV} - G\ I_{VH}}{I_{VV} + 2GI_{VH}}, \quad \text{Where} \quad G = \frac{I_{HV}}{I_{HH}} \tag{1}$$

where G is the instrument correction factor for detector sensitivity to the polarization of the emission, which is 0.7 at the wavelength of detection. $I_{HH}(t)$ and $I_{HV}(t)$ are the intensity of fluorescence decays when the excitation and the emission polarizer are polarized at horizontal-horizontal and horizontal-vertical alignment respectively. Again $I_{VV}(t)$ and $I_{VH}(t)$ are the intensity of fluorescence decays when excitation and emission polarizer are polarized at vertical-vertical and vertical-horizontal alignment respectively. The initial anisotropy values obtained at different temperatures are found to be within the limiting value of 0.4 for both the probe molecules. A representative fluorescence transient from which rotational fluorescence anisotropy has been calculated for C153 in EMIMESU is shown in Fig. 1.

### Time-resolved fluorescence anisotropy study of C153 in ILs

Anisotropy decay profiles of C153 in different room temperature ionic liquids (RTILs) at various temperatures are shown in Fig. 2. The anisotropy decay profiles are fitted to both bi- and single-exponential functions of time. The biexponential fits are found to be slightly better than the single exponential fits. It may be mentioned in this context that Maroncelli and co-workers used a biexponential function to fit the anisotropy decays of C153 in polar solvents, and have explained the observed behavior as a result of the non-Markovian nature of

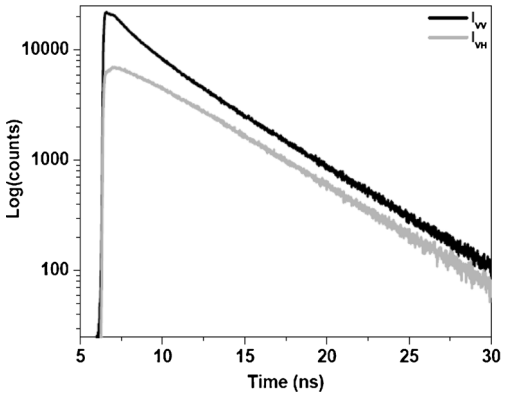


**Fig. 1** The representative fluorescence transient for C153 in EMIMESU at 293 K. $I_{VV}$ and $I_{VH}$ are the intensities of fluorescence decays when excitation and emission polarizer are polarized at vertical-vertical and vertical-horizontal alignment respectively

the friction [42]. The average reorientation times of C153 in the four ionic liquids estimated from biexponential fits at different temperatures are listed in Table 1. The plots of log (η) versus 1/T for the four ionic liquids are also shown in Fig. 3. As can be seen from Fig. 3, these anions play an important role in determining the viscosities of the ILs, and bulk viscosities of the ILs vary in the order TCB<TFB ≅ TFA<ESU.

Interestingly, anisotropy decay profiles (Fig. 2.) reveal that anisotropy decays of C153 is the slowest in EMIMESU and fastest in EMIMTCB. However, anisotropy decays are found to be very similar in case of EMIMTFA and EMIMTFB. Consequently, the average rotational time of C153 in these ILs also follow similar trend (Table 1). For example, at 293 K, the average rotational time of C153 in EMIMESU and EMIMTCB are found to be 3.28 ns and 1.17 ns respectively, whereas the average rotational time of C153 in case of EMIMTFB and EMIMTFA is found to be ~2.05 ns (Table 1). The observation shows that the average rotational times of the probe molecule vary with the bulk viscosities of the ILs. It is also evident both from the anisotropy decay profiles shown in Fig. 2 and the data presented in Table 1 that with an increase in the temperature, the rotational diffusion becomes faster due to the lowering of the viscosity of the media.

We have also analyzed our experimental data by the most commonly used Stokes-Einstein-Debye (SED) hydrodynamic theory of rotational diffusion, according to which the rotational time ($\tau_r^{SED}$) of non-interacting solute in a solvent continuum of viscosity $\eta$ is given by

$$\tau_r^{SED} = \frac{V_h \eta}{k_B T} \tag{2}$$

where $k_B$ is the Boltzmann constant, $T$ is the absolute temperature, $V_h$ is the hydrodynamic volume of the solute molecule with $V_h = VfC$ , V denoting the van der Waals volume of the solute molecule, $f$ the shape factor and $C$ the boundary condition parameter respectively.

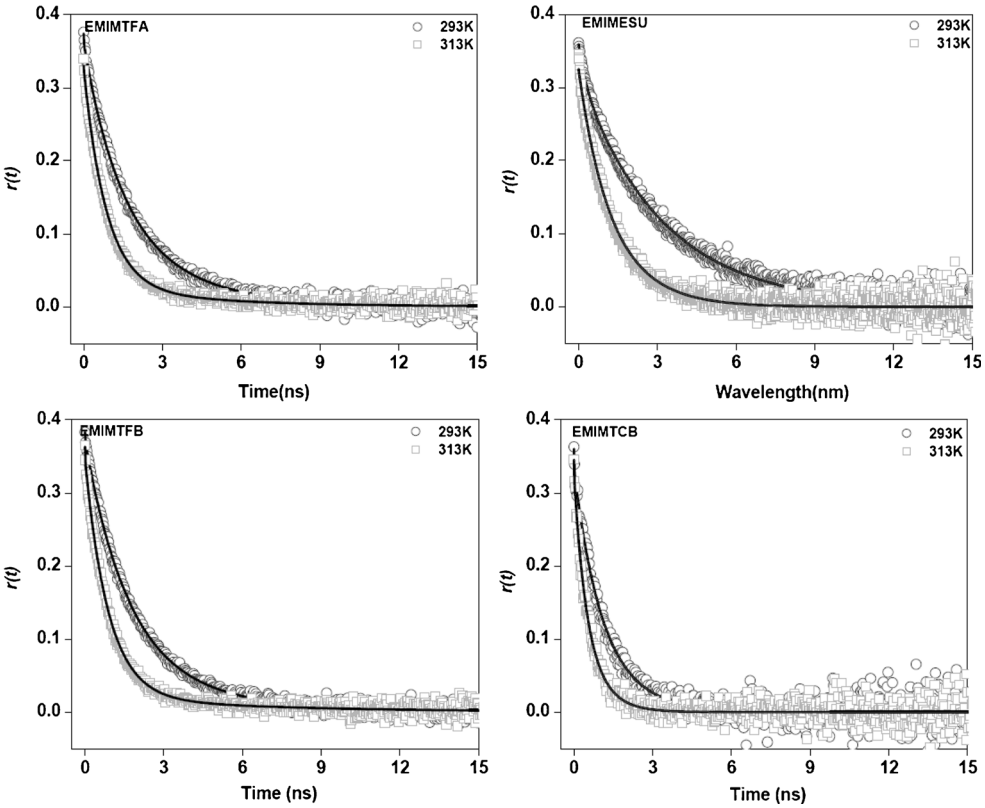


**Fig. 2** Time resolved fluorescence anisotropy decay (TRFAD) profiles of C153 in different RTIL at different temperatures. Symbols denote experimental data points and solid lines passing to the experimental data points represent the biexponential fit to the data points

The two limiting cases are the hydrodynamic stick and slip [41]. When the size of the rotating solute is much bigger than the solvent molecule, $C$ is unity. It is represented as the stick boundary condition. In the case of a solute comparable or smaller than the size of solvent molecule, C is less than unity for which $\tau_r^{SED}$ calculated by Eq. (2), represents only the

**Table 1** Rotational relaxation parameters for C153 in ILs at different temperatures

| ILs | temp.(K) | Viscosity[a] (cP) | [b]$r_0$ | $a_1$ | $\tau_1$ | $a_2$ | $\tau_2$ | $<\tau_{rot}>$ (ns)[c] |
|---|---|---|---|---|---|---|---|---|
| EMIMESU | 293 | 105 | 0.36 | 0.88 | 3.66 | 0.12 | 0.46 | 3.28 |
| | 298 | 75 | 0.36 | 0.81 | 3.34 | 0.19 | 0.90 | 2.88 |
| | 303 | 58 | 0.36 | 0.71 | 2.73 | 0.29 | 1.00 | 2.23 |
| | 308 | 46 | 0.34 | 0.79 | 2.10 | 0.21 | 0.71 | 1.81 |
| | 313 | 34 | 0.34 | 0.81 | 1.63 | 0.19 | 0.36 | 1.39 |
| EMIMTFA | 293 | 38 | 0.37 | 0.18 | 4.19 | 0.82 | 1.57 | 2.04 |
| | 298 | 31 | 0.37 | 0.17 | 4.12 | 0.83 | 1.30 | 1.78 |
| | 303 | 26 | 0.36 | 0.10 | 4.82 | 0.90 | 1.17 | 1.53 |
| | 308 | 22 | 0.36 | 0.08 | 4.89 | 0.92 | 1.04 | 1.35 |
| | 313 | 18 | 0.36 | 0.09 | 4.46 | 0.91 | 0.86 | 1.18 |
| EMIMTCB | 293 | 21 | 0.36 | 0.76 | 1.00 | 0.24 | 1.70 | 1.17 |
| | 298 | 17 | 0.36 | 0.74 | 0.95 | 0.26 | 1.03 | 0.97 |
| | 303 | 14 | 0.36 | 0.77 | 0.71 | 0.23 | 1.20 | 0.82 |
| | 308 | 12 | 0.36 | 0.72 | 0.78 | 0.28 | 0.43 | 0.68 |
| | 313 | 10 | 0.32 | 0.45 | 0.79 | 0.55 | 0.43 | 0.59 |
| EMIMTFB | 293 | 39 | 0.38 | 0.15 | 4.36 | 0.85 | 1.65 | 2.06 |
| | 298 | 32 | 0.36 | 0.07 | 6.58 | 0.93 | 1.47 | 1.83 |
| | 303 | 26 | 0.35 | 0.08 | 4.84 | 0.92 | 1.24 | 1.53 |
| | 308 | 22 | 0.36 | 0.06 | 6.14 | 0.94 | 1.08 | 1.38 |
| | 313 | 18 | 0.36 | 0.06 | 6.35 | 0.94 | 0.89 | 1.22 |

[a] ± 5 %, [b] initial anisotropy and [c] average rotational relaxation time (±5 %). $\tau_1$,$\tau_2$ are rotational relaxation time and $a_1$, $a_2$ are the normalized preexponential factors

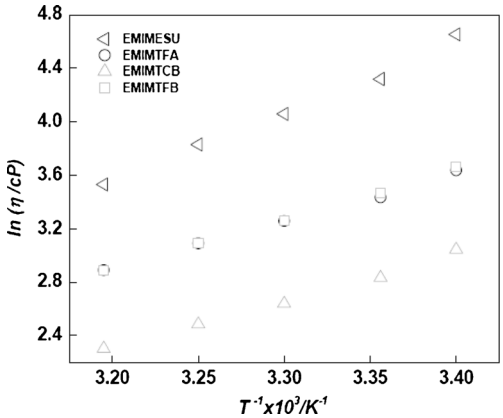


**Fig. 3** Plots of $ln\ (\eta)$ versus $1/T$ for all four RTILs

mechanical or hydrodynamic friction expected by the solute molecule.

For the calculation of the $\tau_r^{SED}$ values, we have used the probe property values that are available in the literatures [17] (Table 2). The values for the probe molecules are given in the Table 2. Since all three axial radii are different, each solute molecule is treated as an asymmetric ellipsoid. The friction coefficient ($\xi_i$) along the three principle axes of rotation for the stick and slip boundary condition are obtained from the literature [43, 44]. The diffusion coefficients along the three axes ($D_i$) are calculated by using the following Einstein relation [45].

$$D_i = \frac{k_B T}{\xi_i} \tag{3}$$

Considering that the transition dipole is along the long axis of the molecule, the rotational times are calculated from the diffusion coefficients by the following equation [46]

$$\tau_r = \frac{1}{12}\left(\frac{4D_a + D_b + D_c}{D_a D_b + D_b D_c + D_c D_a}\right) \tag{4}$$

Where, $D_a$, $D_b$ and $D_c$ are the diffusion coefficients along a, b and c axes, respectively. The boundary condition parameters for slip condition, $C_{slip}$, are obtained from the calculated rotational times and other parameters, relating to the probe, from reference 17.

**Table 2** Solute dimensions and van der Waals volumes together with shape factors and boundary condition parameters calculated using the SED hydrodynamic theory

| Solute | Axial radii/Å$^3$ | van der Waals volume/Å$^3$ | Shape factor($f$) | Boundary conditions($C_{slip}$) |
|---|---|---|---|---|
| C153 | 6.0×3.9×2.5 | 243 | 1.5 | 0.18 |
| AP | 5.0×3.5×1.8 | 134 | 1.6 | 0.16 |

Figure 4 shows the plots of experimentally measured reorientation times of C153 in four ionic liquids along with the calculated stick and slip lines. As can be seen from Fig. 4, the rotational dynamics of C153 in different ILs lie between the stick and slip boundary conditions. We fit the $\tau_r$ and $\eta/T$ data for C153 to the function, $\tau_r = A(\eta/T)^P$, a procedure described by Mali et al. [28, 29] , following relationship are obtained

C153 in EMIMESU

$$\tau_r = (7.042 \pm 0.76)(\eta/T)^{0.70\pm0.074} (\mathrm{N} = 5, \mathrm{R} = 0.9857)$$

C153 in EMIMTFA

$$\tau_r = (8.30 \pm 0.32)(\eta/T)^{0.68\pm0.016} \quad (N = 5, R = 0.992)$$

C153 in EMIMTCB

$$\tau_r = (11.25 \pm 0.82)(\eta/T)^{0.85\pm0.024} \quad (N = 5, R = 0.9988)$$

C153 in EMIMTFB

$$\tau_r = (7.55 \pm 0.44)(\eta/T)^{0.64\pm0.025} \quad (N = 5, R = 0.9978)$$

In these expressions, $N$ and $R$ are the number of data points and regression coefficient, respectively.

We have also calculated the rotational coupling constant ($C_{rot}$) defined as, $C_{rot} = \tau_{rot}/\tau_{stk}$ , where $\tau_{rot}$ is experimental measured rotational time and $\tau_{stk}$, the value obtained by using Eq. 2. The calculated average $C_{rot}$ values obtained for C153 in ESU, TFA, TCB and TFB systems are 0.43, 0.68, 0.66 and 0.68 respectively. $C_{rot}$ values vary from 0.4 to 0.7 which is comparable to the values that obtained in conventional solvents [42]. The observed $C_{rot}$ values also indicate that there is no specific interaction between C153 and the ILs. Moreover, the differences in $C_{rot}$ values that has been observed in the present case on going from one ionic liquid to another

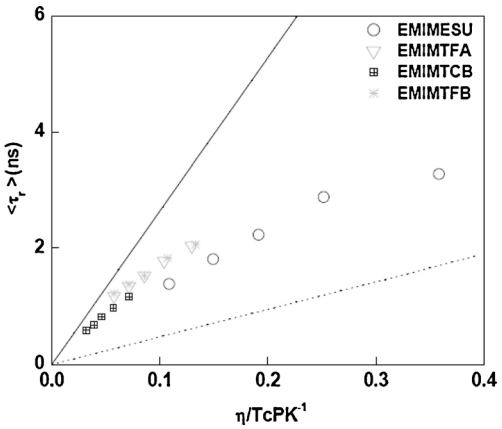


**Fig. 4** Plots for $\tau_r$ vs. $\eta/T$ for C153 in different RTILs. Computed data are with stick (—), slip (.....) boundary conditions and experimentally measured data are shown by symbol

indicates the possible role of nonspecific interaction (long-range dipole-dipole interaction) and solute/solvent size in addition to the viscosity of the medium.

## Time-resolved fluorescence anisotropy study of AP in ILs

Representative anisotropy decay profiles of AP in neat ILs at various temperatures are shown in Fig. 5. We resort to single-exponential fitting of the anisotropy data of AP as biexponential fit does not improve the quality of data fitting and also the average rotational relaxation time calculated from the biexponential fit is found to be very similar with that obtained from the single-exponential fit. The rotational relaxation parameters for AP in the ILs at different temperatures are collected in Table 3.

From the anisotropy decay profiles, it can be noticed that the rotational motion of AP is the fastest in EMIMTCB and slowest in EMIMESU. Interestingly, the rotational motion of AP is found to be slower in EMIMTFA than in EMIMTFB despite the similar viscosity of the two ILs (Fig. 5). This observation indicates that in addition to the viscosity effect other factor like solute-solvent interaction may play a definite role in controlling the rotational motion of AP in these media. The variation of the average rotational times of AP (i.e. 7.6 ns, 3.7 ns, 1.95 ns and 1.13 ns for EMIMESU, EMIMTFA, EMIMTFB and EMIMTCB respectively at 293 K) bear this fact (Table 3). It is also noticeable from Table 3 that with an increase in the temperature, the rotational diffusion of AP becomes faster due to the lowering of the viscosity of the medium. To get a better understanding of the rotational behavior of AP in the ILs, we have also analyzed the data by employing Stokes-Einstein-Debye (SED) hydrodynamic model. In case of AP, Fig. 6 represents the plots of experimentally measured reorientation times of AP in four ionic liquids along with the calculated stick and slip lines. As can be seen from Fig. 6, the rotational time of the AP is significantly higher than that predicted by the stick boundary condition in EMIMESU and EMIMTFA. This kind of behavior is known as "superstick" behavior, which indicates the strong association of the probe molecule with the solvent [15]. Here, we note that a recent study by Khara and Samanta [34] have demonstrated that ethidium bromide (EB) follows superstck behavior in [bmim][TFB] by virtue of solute-solvent hydrogen bonding interaction. Again, Kurnikova et al. [47] has also pointed the role of hydrogen bonding interaction in explaining the superstick behavior of thionine in dimethylsulfoxide (DMSO). The super stick behavior of AP in the present ionic liquids can be attributed to the hydrogen bonding interaction between AP and the ionic liquid. Moreover, the ability of AP to act as H-bond donor is also demonstrated by Dobek and co-workers [48]. They have found that AP can form hydrogen bond (N-H•••O-S) with hydrogen bond acceptors like dimethyl sulfoxide (DMSO) and sodium dodecyl sulfate (SDS). It is pertinent to mention in this context that as the $C_2$-H proton of the EMIM cation is acidic in nature and hence there is a possibility that it may form hydrogen bond with the carbonyl group of AP. However, we could not find any appreciable

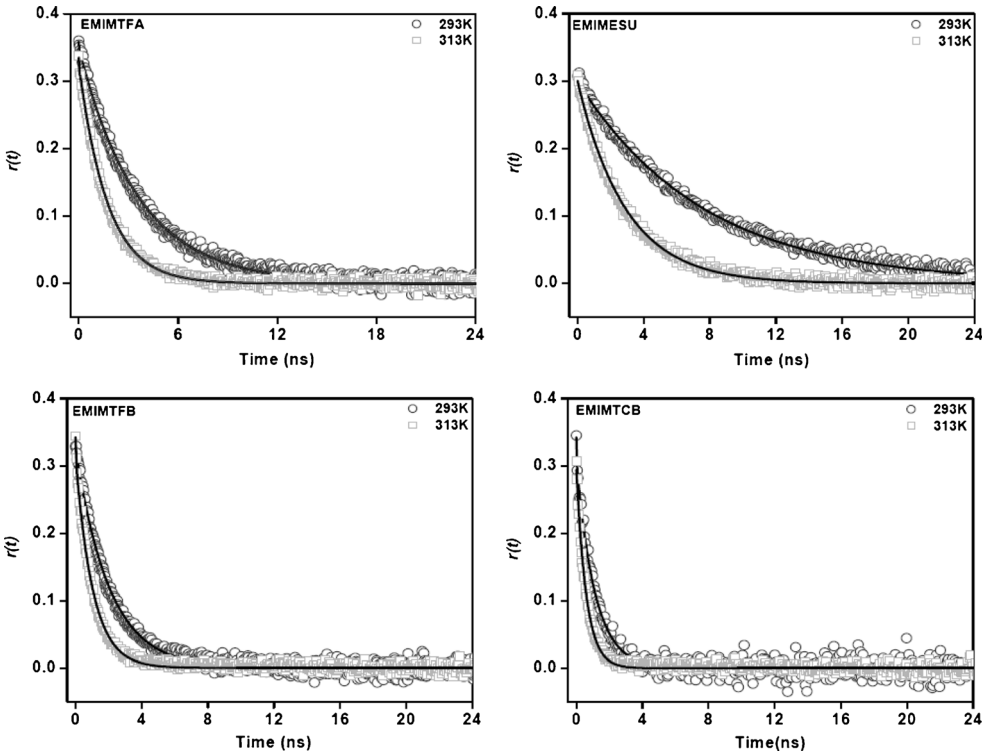


**Fig. 5** Time resolved fluorescence anisotropy decays (TRFAD) of AP in different RTILs at different temperatures. The smooth lines passing to the experimental data points are fitted ones

**Table 3** Rotational relaxation parameters for AP in ILs at different temperatures

| ILs | temp.(K) | Viscosity[a] (cP) | $r_0$[b] | $\tau_{rot}$ (ns)[c] |
|---|---|---|---|---|
| EMIMESU | 293 | 105 | 0.33 | 7.60 |
| | 298 | 75 | 0.32 | 5.77 |
| | 303 | 58 | 0.30 | 4.67 |
| | 308 | 46 | 0.29 | 3.74 |
| | 313 | 34 | 0.29 | 3.00 |
| EMIMTFA | 293 | 38 | 0.36 | 3.70 |
| | 298 | 31 | 0.34 | 3.00 |
| | 303 | 26 | 0.35 | 2.50 |
| | 308 | 22 | 0.35 | 2.10 |
| | 313 | 18 | 0.33 | 1.80 |
| EMIMTCB | 293 | 21 | 0.34 | 1.13 |
| | 298 | 17 | 0.31 | 0.96 |
| | 303 | 14 | 0.31 | 0.82 |
| | 308 | 12 | 0.31 | 0.70 |
| | 313 | 10 | 0.31 | 0.60 |
| EMIMTFB | 293 | 39 | 0.36 | 1.95 |
| | 298 | 32 | 0.34 | 1.65 |
| | 303 | 26 | 0.33 | 1.40 |
| | 308 | 22 | 0.34 | 1.13 |
| | 313 | 18 | 0.32 | 0.95 |

[a] ±5 %, [b] Initial anisotropy and [c] rotational relaxation time (±5 %)

change in the NMR proton signal of $C_2$-H of EMIM cation upon the addition of AP in a separate study [27]. This observation rules out the possibility of the involvement of $C_2$-H proton in the hydrogen bonding interaction with AP. Figure 6 also reveals that AP follows the stick hydrodynamics in EMIMTCB and EMIMTFB. The relationship that has been obtained when we fit $\tau_r$ and $\eta/T$ for AP to the function $\tau_r = A(\eta/T)^p$ are given below

AP in EMIMESU

$$\tau_r = (17.10 \pm 0.28)(\eta/T)^{0.79\pm0.011} \quad (N = 5,\ R = 0.9997)$$

AP in EMIMTFA

$$\tau_r = (23.87 \pm 1.37)(\eta/T)^{0.91\pm0.025} \quad (N = 5,\ R = 0.9995)$$

AP in EMIMTCB

$$\tau_r = (8.88 \pm 0.54)(\eta/T)^{0.78\pm0.021} (N = 5,\ R = 0.9992)$$

AP in EMIMTFB

$$\tau_r = (10.95 \pm 0.97)(\eta/T)^{0.85\pm0.038} \quad (N = 5,\ R = 0.9970)$$

In these expressions, $N$ and $R$ are the number of data points and regression coefficient, respectively

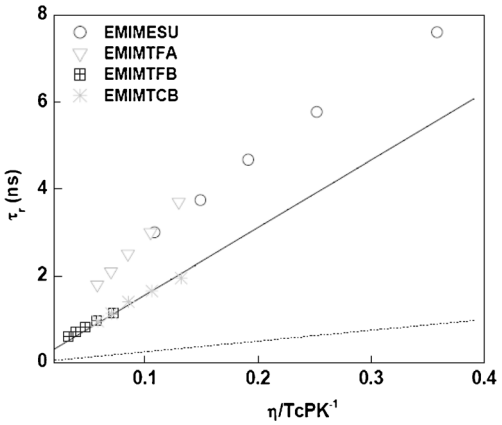


**Fig. 6** Plots for $\tau_r$ vs. $\eta/T$ for AP in different RTILs. Computed data are with stick (—), slip (.....) boundary conditions and experimentally measured data are shown by symbol

To get an insight into the AP-IL interaction, we have estimated the rotational coupling constants for AP in all four ILs used in this study (Table 4). At a particular temperature, $C_{rot}$ values for AP are found to be considerably larger than the ones for non-hydrogen-bonding solvents [17]. Since the rotational coupling constant ($C_{rot}$) represents the measure of the extent of departure from normal hydrodynamic behavior of a solute due to specific interaction, the present observation is a clear manifestation of hydrogen bonding interaction between AP and anionic components of the ionic liquids. Upon careful observation, one can see that $C_{rot}$ values are different for different ILs. The variation of $C_{rot}$ value can be explained by considering hydrogen bond basicity of the corresponding anions of the ILs. The hydrogen bond basicity corresponding to the anions of the concerned ILs are obtained from the literature report [8]. The hydrogen bond basicity of the anions is calculated based on COSMO-RS computation [8]. As described by Klamt [49], COSMO-RS is a statistical thermodynamic approach based on the results of quantum chemical-COSMO calculations. COSMO sigma-moments are molecular descriptors obtained from COSMO-RS calculation, among which the hydrogen bond moments (HB_acc3) chemically corresponds to the measures of H-bonding basicity [8]. As

**Table 4** Rotational coupling constant($C_{rot}$) of AP, obtained from the measured rotation times in four ILs and hydrogen bond basicity parameters for the anions of corresponding ILs

| ILs | $C_{rot}$ for AP | HB_acc3[a] for anion |
|---|---|---|
| EMIMESU | 1.56 | 19.2952 |
| EMIMTFA | 1.90 | 20.3944 |
| EMIMTCB | 1.12 | 3.4554 |
| EMIMTFB | 1.01 | 2.4740 |

[a] COSMO-RS descriptor of HB_acc3 (hydrogen bonding acceptors moment indicates hydrogen bond basicity) [8]

can be seen from Table 4 that observed $C_{rot}$ values for AP (TFA>ESU>TCB>TFB) follows the similar trend to that of hydrogen bond basicity values (TFA>ESU>TCB>TFB) of the corresponding ILs. In this context we would also like to note that very recently, Karve and Dutt [32] have studied the rotational diffusion of neutral and charged solutes in the series of ionic liquids that are different from the present study. They have found that the rhodamine 110 follows stick hydrodynamics, and the variation in the boundary condition parameter can be correlated with the hydrogen bond basicities of the anions of the ILs. Considering all these, one can now conclude that the strength of specific solute-solvent interaction, which in turn is governed by the hydrogen bond basicity of the concerned anions, plays a key role in controlling the dynamics of rotation of the organic solutes in ionic liquids.

## Conclusion

Rotational diffusion of C153 and AP has been investigated in 1-ethyl-3methylimidazolium cation containing ionic liquids with the variation of anions to examine whether the reorientation of solutes is influenced by the nature of anions of the ionic liquid. It has been observed that the reorientation times of C153 depends upon the viscosity of the ionic liquids and follows normal hydrodynamics. The variation in $C_{rot}$ values that has been observed for C153 in ILs also indicates the role of nonspecific interaction (long-range dipole-dipole interaction) and solute/solvent size towards the rotational motion of the probe. On the contrary, the rotational diffusion of AP has been found to be significantly influenced by the nature of anions. AP shows superstick behavior in EMIMESU and EMIMTFA and follows stick hydrodynamics in EMIMTFB and EMIMTCB. The superstick behavior is attributed to the strong specific solute solvent interaction. Rotational coupling constant values for AP are found to decrease in the order TFA>ESU>TCB>TFB. The variation in the rotational coupling constants, the measure of extent of departure from the normal hydrodynamics behavior due to specific solute-solvent interaction, is explained by considering the hydrogen bond basicity of the anionic moiety of the corresponding ILs.

**Acknowledgements** M.S. thanks the Department of Science and Technology (DST) for generous research grant. S.K.D is thankful to Council of scientific and Industrial Research (CSIR) for a fellowship.

## References

1. Welton T (1999) Room-temperature ionic liquids: Solvents for synthesis and catalysis. Chem Rev 99:2071–2084
2. Sheldon R (2001) Catalytic reactions in ionic liquids. Chem Commun 2399–2407. doi:10.1039/B107270F
3. Wasserscheid P, Keim W (2000) Ionic liquids—new "solutions" for transition metal catalysis. Angew Chem Int Ed 39:3772–3789
4. Rogers RD, Voth GA (2007) Ionic liquids. Acc Chem Res 40:1077–1078
5. Weingrätner H (2008) Understanding ionic liquids at the molecular level: Facts, problems, and controversies. Angew Chem Int Ed 47:654–670
6. Rantwijk FV, Sheldon R (2007) Biocatalysis in ionic liquids. Chem Rev 107:2757–2785
7. Rogers RD, Seddon KR (2003) Ionic liquids-solvents of the future? Science 302:792–793
8. Guo Z, Lue BM, Thomasen K, Meyer AS, Xu X (2007) Predictions of flavonoid solubility in ionic liquids by COSMO-RS: Experimental verification, structural elucidation, and solvation characterization. Green Chem 9:1362–1373
9. Masaki T, Nishikawa K, Shirota H (2010) Microscopic study of ionic liquid−$h_2o$ systems: Alkyl-group dependence of 1-alkyl-3-methylimidazolium cation. J Phys Chem B 114:6323–6331
10. Fukazawa H, Ishida T, Shirota H (2011) Ultrafast dynamics in 1-butyl-3-methylimidazolium-based ionic liquids: A femtosecond raman-induced kerr effect spectroscopic study. J Phys Chem B 115:4621–4631
11. Mandal PK, Sarkar M, Samanta A (2004) Excitation-wavelength-dependent fluorescence behavior of some dipolar molecules in room-temperature ionic liquids. J Phys Chem A 108:9048–9053
12. Paul A, Samanta A (2007) Solute rotation and solvation dynamics in an alcohol-functionalized room temperature ionic liquid. J Phys Chem B 111:4724–4731
13. Paul A, Samanta A (2008) Effect of nonpolar solvents on the solute rotation and solvation dynamics in an imidazolium ionic liquid. J Phys Chem B 112:947–953
14. Samanta A (2010) Solvation dynamics in ionic liquids: what we have learned from the dynamic fluorescence stokes shift studies. J Phys Chem Lett 1:1557–1562
15. Ingram JA, Moog RS, Ito N, Biswas R, Maroncelli M (2003) Solute rotation and solvation dynamics in a room-temperature ionic liquid. J Phys Chem B 107:5926–5932
16. Ito N, Arzhantsev S, Heitz M, Maroncelli M (2004) Solvation dynamics and rotation of coumarin 153 in alkylphosphonium ionic liquids. J Phys Chem B 108:5771–5777
17. Ito N, Arzhantsev S, Maroncelli M (2004) The probe dependence of solvation dynamics and rotation in the ionic liquid 1-butyl-3-methyl-imidazolium hexafluorophosphate. Chem Phys Lett 396:83–91
18. Arzhantsev S, Jin H, Baker GA, Maroncelli M (2007) Measurements of the complete solvation response in ionic liquids. J Phys Chem B 111:4978–4989
19. Jin H, Baker GA, Arzhantsev S, Dong J, Maroncelli M (2007) Solvation and rotational dynamics of coumarin 153 in ionic liquids: Comparisons to conventional solvents. J Phys Chem B 111:7291–7302
20. Seth D, Sarkar S, Sarkar N (2008) Solvent and rotational relaxation of coumarin 153 in a protic ionic liquid dimethylethanolammonium formate. J Phys Chem B 112:2629–2636
21. Sarkar S, Pramanik R, Ghatak C, Setua P, Sarkar N (2010) Probing the interaction of 1-ethyl-3-methylimidazolium ethyl sulfate ([emim][$etso_4$]) with alcohols and water by solvent and rotational relaxation. J Phys Chem B 114:2779–2789
22. Daschakraborty S, Biswas R (2011) Stokes shift dynamics in (ionic liquid+polar solvent) binary mixtures: Composition dependence. J Phys Chem B 115:4011–4024
23. Daschakraborty S, Biswas R (2011) Stokes' shift dynamics in alkylimidazolium aluminate ionic liquids: Domination of solute-IL dipole–dipole interaction. Chem Phys Lett 510:202–207
24. Das SK, Sarkar M (2011) Solvation and rotational relaxation of coumarin 153 and 4-aminophthalimide in a new hydrophobic ionic liquid: Role of N–H. . . F interaction on solvation dynamics. Chem Phys Lett 515:23–28

25. Das SK, Sarkar M (2012) Solvation and rotational relaxation of coumarin 153 in a new hydrophobic ionic liquid: An excitation wavelength dependence study. J Lumi 132:368–374
26. Das SK, Sarkar M (2011) Steady-state and time-resolved fluorescence behavior of coumarin-153 in a hydrophobic ionic liquid and ionic liquid–toluene mixture. J Mol Liq 165:38–43
27. Das SK, Sarkar M (2012) Rotational dynamics of coumarin-153 and 4-aminophthalimide in 1-ethyl-3-methylimidazolium alkylsulfate ionic liquids: effect of alkyl chain length on the rotational dynamics. J Phys Chem B 116:194–202
28. Mali KS, Dutt GB, Mukherjee T (2005) Do organic solutes experience specific interactions with ionic liquids? J Chem Phys 123: 174504
29. Mali KS, Dutt GB, Mukherjee T (2008) Rotational diffusion of a nonpolar and a dipolar solute in 1-butyl-3-methylimidazolium hexafluorophosphate and glycerol: Interplay of size effects and specific interactions. J Chem Phys 128:054504
30. Dutt GB (2010) Influence of specific interactions on the rotational dynamics of charged and neutral solutes in ionic liquids containing tris(pentafluoroethyl)trifluorophosphate (FAP) anion. J Phys Chem B 114:8971–8977
31. Karve L, Dutt GB (2011) Rotational diffusion of neutral and charged solutes in ionic liquids: is solute reorientation influenced by the nature of the cation? J Phys Chem B 115:725–729
32. Karve L, Dutt GB (2012) Rotational diffusion of neutral and charged solutes in 1-butyl-3-methylimidazolium-based ionic liquids: influence of the nature of the anion on solute rotation. J Phys Chem B 116:1824–1830
33. Fruchey K, Fayer MD (2010) Dynamics in organic ionic liquids in distinct regions using charged and uncharged orientational relaxation probes. J Phys Chem B 114:2840–2845
34. Khara DC, Samanta A (2010) Rotational dynamics of positively and negatively charged solutes in ionic liquid and viscous molecular solvent studied by time-resolved fluorescence anisotropy measurements. Phys Chem Chem Phys 12:7671–7677
35. Khara DC, Samanta A (2012) Fluorescence response of coumarin-153 in *n*-alkyl-*n*-methylmorpholinium ionic liquids: are these media more structured than the imidazolium ionic liquids?J. Phys Chem B 116:13430–13438
36. Khara DC, Kumar JP, Mondal N, Samanta A (2013) Effect of the alkyl chain length on the rotational dynamics of nonpolar and dipolar solutes in a series of n-alkyl-n-methylmorpholinium ionic liquids. J Phys Chem B 117:5156–5164
37. Das SK, Sahu PK, Sarkar M (2013) Diffusion–viscosity decoupling in solute rotation and solvent relaxation of coumarin153 in ionic liquids containing fluoroalkylphosphate (FAP) anion: A thermophysical and photophysical study. J Phys Chem B 117:636–647
38. Santhosh K, Banerjee S, Rangaraj N, Samanta A (2010) Fluorescence response of 4-(n, n′-dimethylamino)benzonitrile in room temperature ionic liquids: observation of photobleaching under mild excitation condition and multiphoton confocal microscopic study of the fluorescence recovery dynamics. J Phys Chem B 114: 1967–1974
39. Santhosh K, Samanta A (2010) Modulation of the excited state intramolecular electron transfer reaction and dual fluorescence of crystal violet lactone in room temperature ionic liquids. J Phys Chem B 114:9195–9200
40. Dutt GB (2005) Molecular rotation as a tool for exploring specific solute–solvent interaction. ChemPhyChem 6:413–418
41. Hu CM, Zwanzig R (1974) Rotational friction coefficients for spheroids with the slipping boundary condition. J Chem Phys 60:4354
42. Horng ML, Gardecki J, Maroncelli M (1997) Rotational dynamics of coumarin 153: Time-dependent friction, dielectric friction, and other nonhydrodynamic effects. J Phys Chem A 101:1030–1047
43. Small EW, Isenberg I (1977) Hydrodynamic properties of a rigid molecule: Rotational and linear diffusion and fluorescence anisotropy. Biopolymers 16:1907–1928
44. Sension RJ, Hochstrasser RM (1993) Comment on: Rotational friction coefficients for ellipsoids and chemical molecules with slip boundary conditions. J Chem Phys 98:2490
45. Valeur B (2002) Molecular fluorescence, principles and applications. Wiley-VCH, Weinheim (FRG), Chapter 8
46. Hartman RS, Alavi DS, Waldeck DH (1991) An experimental test of dielectric friction models using the rotational diffusion of aminoanthraquinones. J Phys Chem 95:7872–7880
47. Kurnikova MG, Balabai N, Waldeck DH, Coalson RD (1998) Rotational relaxation in polar solvents: Molecular dynamics study of solute−solvent interaction. J Am Chem Soc 120:6121–6130
48. Maciejewski A, Kubicki J, Dobek K (2003) The origin of time-resolved emission spectra (tres) changes of 4-aminophthalimide (4-ap) in SDS micelles: the role of the hydrogen bond between 4-ap and water present in micelles. J Phys Chem B 107:13986–13999
49. Klamt A (1995) Conductor-like screening model for real solvents: A new approach to the quantitative calculation of solvation phenomena. J Phys Chem 99:2224–2235